PROCEEDINGS OF SCIENCE

CP violation with $B_s^0 \to J/\psi\phi(1020)$ decays in CMS

Giacomo Fedi
on behalf of the CMS Collaboration
Imperial College, London, UK
E-mail: giacomo.fedi@cern.ch

We presented the most recent results obtained by the CMS Collaboration on the measurement of the CP-violating phase ϕ_s using the $B_s^0 \to J/\psi\phi(1020)$ decay channel in the data collected at $\sqrt{s}$ =13 TeV with a muon-enriching trigger in the 2017 and the 2018 data-taking years. The fit over a data sample of an integrated luminosity of 96.4 fb^{-1} yielded $\phi_s = -11 \pm 50\,(\text{stat}) \pm 10\,(\text{syst})$ mrad and $\Delta\Gamma_s = 0.114 \pm 0.014\,(\text{stat}) \pm 0.007\,(\text{syst})$ ps^{-1}. Those results are also combined with previous CMS measurements at $\sqrt{s} = 8$ TeV, obtaining $\phi_s = -21 \pm 45$ mrad and $\Delta\Gamma_s = 0.1073 \pm 0.0097$ ps^{-1}. Both results are in agreement with the standard model predictions.

BEAUTY2020
21-24 September 2020
Kashiwa, Japan (online)

PoS(BEAUTY2020)014

1. Introduction

The weak CP-violating phase ϕ_s is a phase that stems from the interference between B_s^0 decays proceeding directly and through B_s^0-$\overline{B}_s^0$ mixing to a CP final state. The standard model (SM) prediction is close to zero and precisely predicted as $\phi_s \simeq -2\beta_s = arg(-V_{ts}V_{tb}^*/V_{cs}V_{cb}^*) = -36.96^{+0.72}_{-0.84}$ mrad [2], where V_{xy} are the elements of the CKM matrix and β_s is one of the angles of the unitarity triangles. The ϕ_s phase is measured reconstructing the $B_s^0 \to J/\psi\phi(1020)$ decay channel. The $B_s^0 \to J/\psi\phi(1020)$ decay is a golden channel to search for New Physics in the β_s CP-violating weak phase. The CP-violating weak phase can vary up to $\sim$ 10% in case of new particles contributing to the B_s^0-$\overline{B}_s^0$ mixing [3].

2. Methodology

Using data collected by the CMS experiment [4], the CP-violating phase ϕ_s is measured. The data sample of an integrated luminosity of 96.4 fb^{-1} is composed of a selection of $B_s^0 \to J/\psi\phi(1020)$ candidates obtained from LHC proton-proton collisions at $\sqrt{s}$ =13 TeV with a muon-enriching trigger in the 2017 and 2018 data-taking years [1].

The $B_s^0 \to J/\psi\phi(1020)$ decay channel is studied reconstructing the J/ψ in the $\mu\mu$ decay channel and the $\phi(1020)$ in the K^+K^- decay channel. A selection on the kinematic variables and on the proper decay time of the B_s^0 decay products is applied to increase the signal to background ratio. A total number of 48,500 B_s^0 candidates is reconstructed as signal events.

In order to properly and efficiently measure the ϕ_s weak phase in the $B_s^0 \to J/\psi\phi(1020)$ decay channel different observables are used: the B_s^0 mass, the B_s^0 proper decay time ct and its uncertainty σ_{ct}, the decay angles of the decay products (θ_T,ψ_T,ϕ_T), the charge (flavour) of the B_s^0 at production time, and the mistag ratio ω_{tag}, which accounts for the level of reliability of the flavour information.

The analysis employs two techniques to increase the sensitivity on ϕ_s: a dedicated tagging trigger, which requires the presence of three muons in the event, two for the J/ψ reconstruction and one for the flavour tagging, and a novel opposite-side muon flavor tagger based on Deep Neural Networks (DNN). Taken together, these two improvements increase the muon tagging performance by ≈20% compared to that in Ref. [5], while the effect of muon enriching of the trigger increases the tagging muon efficiency ϵ_{tag} by a factor ≈10. The mistag ratio ω_{tag} is measured by the DNN in a per-event fashion and is inferred in data by the DNN using a number of kinematic variables of the muon and its geometrical position with respect to the the signal-background particles. The response of the DNN is optimised using simulations of the signal and is calibrated in each year of data-daking using the self-tagging channel $B^+ \to J/\psi K^+$. The results of the calibration of the mistag ratio ω_{tag} are shown in Fig. 1. The performance of the muon flavour tagger, summarised in Table 1, is evaluated by the tagging power which is defined as $P_{tag} = \epsilon_{tag}(1 - 2\omega_{tag})^2$.

The ϕ_s weak phase is measured along with a number of other physics parameters such as the decay width difference $\Delta\Gamma_s$ between the light and heavy B_s^0 meson mass eigenstates; the magnitudes of the perpendicular, longitudinal, and parallel transversity amplitudes of the $B_s^0 \to J/\psi\phi(1020)$ decay ($|A_\perp|^2$, $|A_0|^2$, and $|A_\parallel|^2$ respectively); the magnitude $|A_S|^2$ of the S-wave amplitude from $B_s^0 \to J/\psi f(980)$ and nonresonant $B_s^0 \to J/\psi K^+K^-$ decays; the strong phases parameters $\delta_\perp$, δ_0, $\delta_\parallel$, and δ_S associated with the interference between the amplitudes; the decay rate Γ_s; the mass

Table 1: Calibrated opposite-side muon tagger performance evaluated using $B^+ \to J/\psi K^+$ events in the 2017 and 2018 data samples. The uncertainties shown are statistical only.

Data sample	ϵ_{tag} (%)	ω_{tag} (%)	P_{tag} (%)
2017	45.7 ± 0.1	27.1 ± 0.1	9.6 ± 0.1
2018	50.9 ± 0.1	27.3 ± 0.1	10.5 ± 0.1

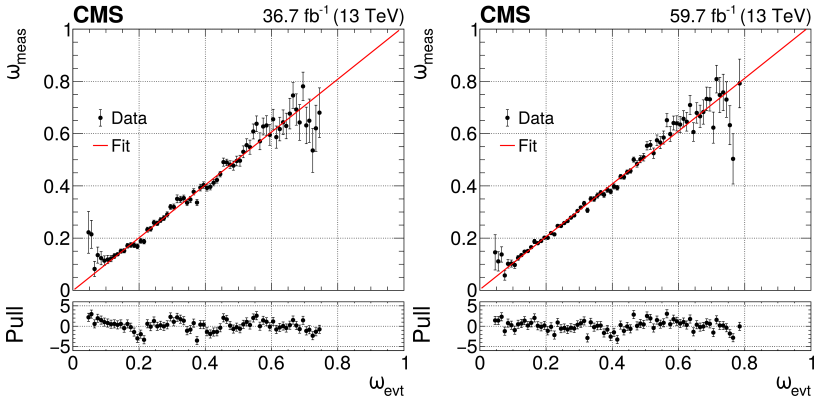

Figure 1: Results of the calibration of the per-event mistag probability ω_{evt} based on $B^+ \to J/\psi K^+$ decays from the 2017 (left) and 2018 (right) data samples [1]. The vertical bars represent the statistical uncertainties. The solid line shows a linear fit to data (solid markers). The pull distributions between the data and the fit function in each bin are shown in the lower panels.

difference Δm_s between the two B_s^0 meson mass eigenstates; and $|\lambda|$ which accounts for possible contributions from the direct CP violation in the $B_s^0 \to J/\psi\phi(1020)$ decay.

The physics parameters are fitted on the data samples in a simultaneous fashion using an unbinned multidimensional maximum-likelihood fit. The likelihood function is composed of three components, signal, combinatorial background, and peaking background.

The signal component is equivalent to the one used in the previous CMS analysis [5]. In the present analysis all the parameters of interest are left free to float. The effect of the detector on the proper decay time ct and the angular variables is unfolded including efficiency functions in the model. The efficiency functions are measured in simulated signal samples. The proper decay efficiency measurement method is validated by using it to measure the mean lifetime of the $B^\pm$ in the $B^+ \to J/\psi K^+$ decay channel in data. The mean lifetime of the $B^\pm$ obtained from the fit of different data-taking period samples is compared with the world average value [6], and a good level of agreement is observed. The proper decay time resolution is taken into account with the convolution of the proper decay time function with a Gaussian function. The Gaussian function inputs a per-event resolution which is estimated in data using the proper decay time uncertainty σ_{ct} and a correction factor κ.

The combinatorial background component is composed of arbitrary functions that have demonstrated to fit well the background distributions, both in simulated samples of the main background channels – B-hadrons decaying in inclusive $J/\psi X$ decay channels – and on the events in side-bands of the signal resonance in the B_s^0 mass distribution.

The peaking background component represents the contribution of the $B^0 \to J/\psi K^*$ decay

Table 2: Results of the fit to data.

Parameter	Value	Stat.	Syst.
ϕ_s [mrad]	-11	± 50	± 10
$\Delta\Gamma_s$ [ps^{-1}]	0.114	± 0.014	± 0.007
Γ_s [ps^{-1}]	0.6531	± 0.0042	± 0.0024
Δm_s [$\hbar$ ps^{-1}]	17.51	$^{+0.10}_{-0.09}$	± 0.02
$\lvert\lambda\rvert$	0.972	± 0.026	± 0.008
$\lvert A_0\rvert^2$	0.5350	± 0.0047	± 0.0048
$\lvert A_\perp\rvert^2$	0.2337	± 0.0063	± 0.0044
$\lvert A_S\rvert^2$	0.022	$^{+0.008}_{-0.007}$	± 0.016
$\delta_\parallel$ [rad]	3.18	± 0.12	± 0.03
$\delta_\perp$ [rad]	2.77	± 0.16	± 0.04
$\delta_{S\perp}$ [rad]	0.221	$^{+0.083}_{-0.070}$	± 0.048

channel. The invariant mass distribution of the B^0, reconstructed in the $B^0 \to J/\psi K^*$ decay channel, falls beneath the B_s^0 mass resonance when the $K^* \to K^+\pi^-$ has the pion erroneously given the mass of a kaon. The peaking background functions for each of the fitted variables are obtained using simulations of the $B^0 \to J/\psi K^*$ decay channel.

3. Results

The results of the fit with their statistical and systematic uncertainties are given in Table 2. The distributions of the input parameters and the corresponding fit projections are shown in Figs. 2 and Figs. 3. Several sources of systematic uncertainties in the physics parameters are taken into account by testing the various assumptions made in the fit model and those associated with the fitting procedure. The most relevant systematic uncertainties for ϕ_s and for $\Delta\Gamma_s$ are those associated to the assumptions made on the efficiency functions and on the likelihood function (model bias).

The λ parameter is measured to be $\lambda = 0.972 \pm 0.026\,(\text{stat}) \pm 0.008\,(\text{syst})$, consistent with no direct violation. The measured $\Delta m_s = 17.51\,^{+0.10}_{-0.09}\,(\text{stat}) \pm 0.03\,(\text{syst})$ is consistent with the theoretical prediction $\Delta m_s = 18.77 \pm 0.86$ [7], but in slight tension with the world-average value $\Delta m_s = 17.757 \pm 0.021$ [6].

4. 13 TeV and 8 TeV combined results

The results of the present analysis and the ones of the previous CMS analysis made on the same $B_s^0 \to J/\psi\phi(1020)$ channel at different proton-proton collision energy $\sqrt{s} = 8$ TeV [5] are combined taking into account the correlations among the fitted parameters. Two variables, $|\lambda|$ and Δm_s, are not included in the combination since constraints were applied in the previous analysis. The combined results for the CP-violating phase and the lifetime difference between the two mass eigenstates are:

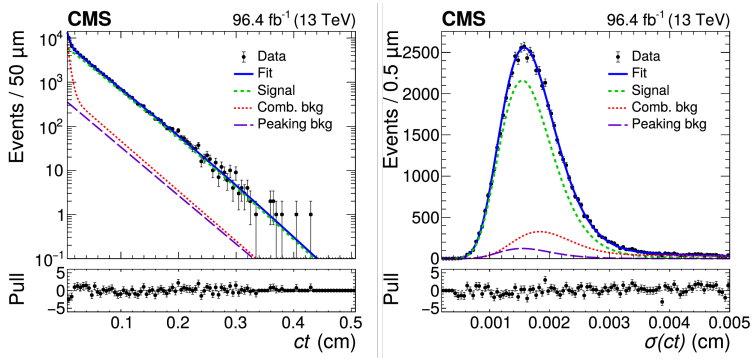

Figure 2: The ct distribution (left) and its uncertainty (right) for the $B_s^0 \to J/\psi\phi(1020)$ candidates in data [1]. The vertical bars on the points represent the statistical uncertainties. The solid line represents a projection of the fit to data, the dashed line corresponds to the signal, the dotted line to the combinatorial background, and the long-dashed line to the peaking background, as obtained from the fit. The distribution of the differences between the data and the fit, divided by the combined uncertainty in the data and the best fit function for each bin (pulls) is displayed in the lower panel.

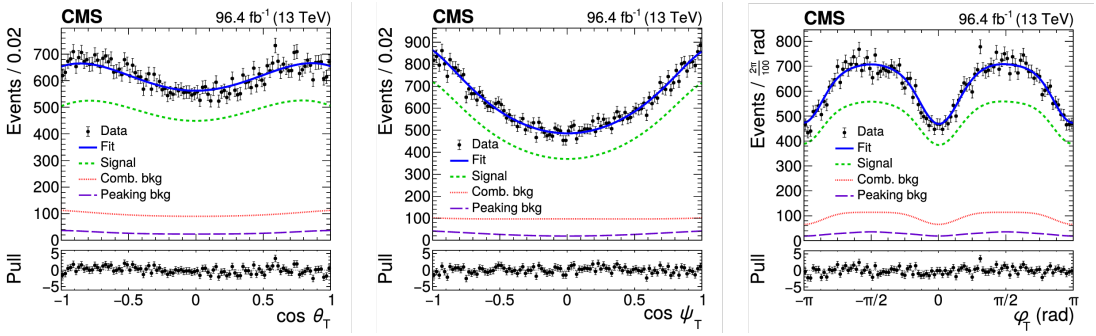

Figure 3: The angular distributions $\cos\theta_T$ (left), $\cos\psi_T$ (middle), and φ_T (right) for the $B_s^0 \to J/\psi\phi(1020)$ candidates and the projections from the fit [1]. The notations are as in Fig. 2.

$$\phi_s = -21 \pm 45\,\text{mrad}$$
$$\Delta\Gamma_s = 0.1073 \pm 0.0097\,\text{ps}^{-1}.$$

The two-dimensional ϕ_s vs. $\Delta\Gamma_s$ likelihood contours at 68% confidence level (CL) for the individual and combined results, as well as the SM prediction [2, 7], are shown in Fig. 4. The contours for the individual results are obtained with likelihood scans, which are used to obtain the combined contour. The results are in agreement with each other and with the SM predictions [2, 7].

5. Conclusions

The CP-violating phase ϕ_s is measured using the $B_s^0 \to J/\psi\phi(1020)$ decay channel in the data collected at $\sqrt{s}$ =13 TeV in the 2017 and the 2018 data-taking years. The fit over a data sample of an integrated luminosity of 96.4 fb^{-1} yielded a CP-violating phase $\phi_s = -11 \pm 50\,(\text{stat}) \pm$

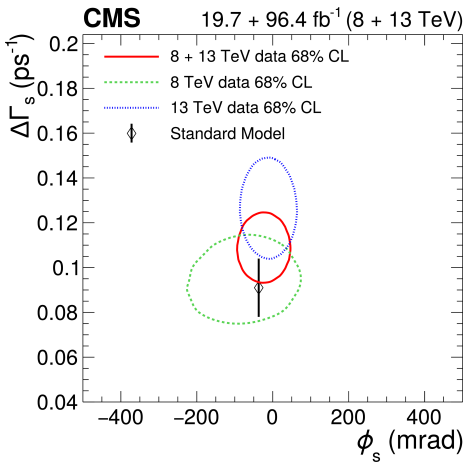

Figure 4: The two-dimensional likelihood contours at 68% CL in the ϕ_s-$\Delta\Gamma_s$ plane, for the CMS 8 TeV (dashed line), 13 TeV (dotted line), and combined (solid line) results [1]. The SM prediction is shown with the diamond marker [2, 7].

10 (syst) mrad and a lifetime difference between the two mass eigenstates $\Delta\Gamma_s = 0.114 \pm 0.014$ (stat)$\pm$ 0.007 (syst) ps^{-1}. The presented results are also combined with those measured by the CMS collaboration at $\sqrt{s}$=8 TeV [5], obtaining $\phi_s = -21 \pm 45$ mrad and $\Delta\Gamma_s = 0.1073 \pm 0.0097$ ps^{-1}. Both results are in agreement with the SM predictions [2, 7].

References

[1] V. Khachatryan *et al.* (CMS Collaboration), "Measurement of the CP violating phase ϕ_s in the $B_s \to J/\psi\,\phi(1020) \to \mu^+\mu^-\,K^+K^-$ channel in proton-proton collisions at $\sqrt{s}$ = 13 TeV," CMS-PAS-BPH-20-001.

[2] J. Charles *et al.* "Predictions of selected flavour observables within the Standard Model," Phys. Rev. D **84** (2011), 033005 doi:10.1103/PhysRevD.84.033005.

[3] C. W. Chiang *et al.*, "New Physics in B0(s) → J/psi phi: A General Analysis," JHEP **04** (2010), 031 doi:10.1007/JHEP04(2010)031.

[4] S. Chatrchyan *et al.* (CMS Collaboration), "The CMS Experiment at the CERN LHC," JINST **3** (2008), S08004 doi:10.1088/1748-0221/3/08/S08004.

[5] V. Khachatryan *et al.* (CMS Collaboration), "Measurement of the CP-violating weak phase ϕ_s and the decay width difference $\Delta\Gamma_s$ using the $B_s^0 \to J/\psi\phi(1020)$ decay channel in pp collisions at $\sqrt{s}$ = 8 TeV," Phys. Lett. B **757** (2016), 97-120 doi:10.1016/j.physletb.2016.03.046.

[6] M. Tanabashi *et al.* [Particle Data Group], "Review of Particle Physics," Phys. Rev. D **98** (2018) no.3, 030001 doi:10.1103/PhysRevD.98.030001.

[7] A. Lenz and G. Tetlalmatzi-Xolocotzi, "Model-independent bounds on new physics effects in non-leptonic tree-level decays of B-mesons," JHEP **07** (2020), 177 doi:10.1007/JHEP07(2020)177.